Supporting Information for

Ultrafast Dynamics of Water-Protein Coupled Motions Around the Surface of Eye Crystallin

Patrick Houston, Nicolas Macro, Minhee Kang, Long Chen, Jin Yang, Lijuan Wang, Zhengrong Wu* and Dongping Zhong*

Department of Physics, Department of Chemistry and Biochemistry, and Programs of Biophysics, Chemical Physics, and Biochemistry, The Ohio State University, Columbus Ohio, 43210, USA

*Corresponding author. E-mail: zhong.28@osu.edu, wu.473@osu.edu

Data Analysis

We fit femtosecond-resolved transients to a sum of exponential decays

$$I_\lambda(t) = I_\lambda^{solv}(t) + I_\lambda^{pop} = \sum_i a_i e^{\frac{-t}{\tau_i}} + (t) \sum_j b_j e^{\frac{-t}{\tau_j}} \quad \text{(S1)}$$

where the first term represents the solvation processes and the second term represents the intrinsic lifetime emission of the tryptophan side chain (population decays). The pre-factor a_i is positive at the blue side of the emission spectrum representing the decay dynamics of the emission peak and may be negative at the red side, representing rise dynamics characteristic of solvation relaxation.

We construct the overall emission spectrum at each time as

$$I(\lambda, t) = \frac{I_{ss}(\lambda) I_\lambda(t)}{\sum_i a_i \tau_i + \sum_j b_j \tau_j} \quad \text{(S2)}$$

where $I_\lambda(t)$ is the time-resolved transient fit at a specific wavelength and $I_{ss}(\lambda)$ is the peak-normalized intensity of the steady-state emission spectrum at that wavelength.

Likewise, we constructed the lifetime associated spectrum as

$$I^{pop}(\lambda, t) = \frac{I_{ss}(\lambda) I_\lambda^{pop}(t)}{\sum_i a_i \tau_i + \sum_j b_j \tau_j} \quad \text{(S3)}$$

We convert both time-resolved spectra to the wavenumber domain and fit by log-normal functions to obtain the time-resolved maxima of both spectra $\left(\nu_s(t), \nu_l(t)\right)$. We then construct the solvation correlation function defined by

$$C(t) = \frac{\nu_s(t) - \nu_l(t)}{\nu_s(0) - \nu_l(0)} \quad \text{(S4)}$$

Finally, we fit the *C(t)* to a multiexponential function and used these parameters to determine the dissipation energies and solvation speeds as detailed in the text.

NMR Methods

We performed NMR T_1, $T_{1\rho}$, and heteronuclear NOE experiments at 298K on Bruker Avanced 800 MHz, 700 MHz, and 600 MHz spectrometers equipped with a cryogenic probe and performed T_1 and heteronuclear NOE experiments according to the pulse sequence introduced by Kay et al.[1] We collected data for $T_{1\rho}$ experiments using the pulse sequence described by the Bax group.[2] We processed data using nmrPipe[3] with T_1 relaxation delays set to 40, 360, 720, 1080, and 1800 ms with two duplicate points for error calculation. We measure $T_{1\rho}$ with a spin lock field strength of 2.0 KHz for a variable relaxation during of 20, 40, 60, 80 and 100 ms.[2] The calculated spin lock frequency was 2000.44 kHz which we calibrated according to methods developed by Palmer et al.[4]

We measured NOE with and without 1.5 sec ^{1}H saturation periods at the beginning of the pulse sequence. Because the magnetization starts from the less sensitive ^{15}N nucleus in NOE measurements, about 94 scans were collected per FID. We derived NOE values from the ratio of peak intensity between the two spectra.

We assigned resonances for all mutants by direct comparisons with the WT HSQC. Ambiguous resonances were left unassigned and excluded from further analysis. We fit signal intensity of each assigned resonance vs. relaxation time with a single exponential decay to derive R_1 and R_2 values using both the MATLAB based DYNAMICS program and JAVA based ROTDIF.[5,6] Both programs provide site-specific dynamic parameters such as S^2, τ_c, τ_{loc}, and R_{ex} from NMR relaxation data.[7] We collected multiple sets of T_1, T_2, and NOE data under different magnetic fields to precisely extract these dynamic parameters. Multiple sets of data allowed us to

fit under the model free formalism with variable values of the chemical shift anisotropy (CSA) tensor.[6]

Molecular Dynamics Simulations

We performed simulations using the GROMACS 2018.2 package[8] using the CHARMM36 all-atom forcefield. We obtained the NMR solution structure from the Protein Data Bank (PDB ID: 2M3C) and performed tryptophan mutations in PyMol, choosing the lowest energy configuration as the initial structure. We solvated the protein with TIP3P water in a 10 angstom dodecahedral box and added one Na^+ ion to neutralize the system. We performed an energy minimization step to relax to the system using the steepest descent algorithm in steps of 1 Å and continuing until the maximum force is less than 1000.0 kJ/mol/nm. The system was then relaxed at a constant volume with periodic boundaries for 100 ps with a step size of 2 fs, raising the temperature to 300K and constraining bonds involving hydrogen atoms with the LINCS algorithm. The system was then relaxed under a constant pressure of 1 bar for 100 ps with a step size of 2 fs. Finally, we obtained trajectories from 30 ns simulations run in three iterations of 10 ns each. These simulations were performed on the Pitzer cluster using resources provided by an Ohio Supercomputer Center grant.

REFERENCES

(1) Kay, L. E.; Torchia, D. A.; Bax, A. Backbone Dynamics of Proteins as Studied by Nitrogen-15 Inverse Detected Heteronuclear NMR Spectroscopy: Application to Staphylococcal Nuclease. *Biochemistry* **1989**, *28* (23), 8972–8979.

(2) Lakomek, N.-A.; Ying, J.; Bax, A. Measurement of 15N relaxation rates in perdeuterated proteins by TROSY-based methods. *J. Biomol. NMR* **2012**, *53* (3), 209–221.

(3) Delaglio, F.; Grzesiek, S.; Vuister, G. W.; Zhu, G.; Pfeifer, J.; Bax, A. NMRPipe: A multidimensional spectral processing system Based on UNIX pipes. *J. Biomol. NMR* **1995**, *6* (3), 277–293.

(4) Palmer, A. G., 3rd; Kroenke, C. D.; Patrick Loria, J. Nuclear Magnetic Resonance Methods for Quantifying Microsecond-to-Millisecond Motions in Biological Macromolecules. In *Methods in Enzymology*; James, T. L., Dötsch, V., Schmitz, U., Eds.; Academic Press, 2001; Vol. 339, pp 204–238.

(5) Fushman, D. Determining protein dynamics from 15N relaxation data by using DYNAMICS. *Methods Mol. Biol.* **2012**, *831*, 485–511.

(6) Berlin, K.; Longhini, A.; Dayie, T. K.; Fushman, D. Deriving Quantitative Dynamics Information for Proteins and RNAs Using ROTDIF with a Graphical User Interface. *J. Biomol. NMR* **2013**, *57* (4), 333–352. https://doi.org/10.1007/s10858-013-9791-1.

(7) Lipari, G.; Szabo, A. Model-free approach to the interpretation of nuclear magnetic resonance relaxation in macromolecules. 1. Theory and Range of Validity. *J. Am. Chem. Soc.* **1982**, *104* (17), 4546–4559.

(8) Abraham, M. J.; Murtola, T.; Schulz, R.; Páll, S.; Smith, J. C.; Hess, B.; Lindahl, E. GROMACS: High performance molecular simulations through multi-level parallelism from laptops to supercomputers. *SoftwareX* **2015**, *1–2*, 19–25.

Table S1. Fitting results of the hydration dynamics for all 9 mutants of γM7.

Mutant	λ_{SS} (nm)	λ_0 (nm)	ΔE_{SS} (cm^{-1})	τ_1 (ps)	A_1	ΔE_1 (cm^{-1})	τ_2 (ps)	A_2	ΔE_2 (cm^{-1})	τ_3 (ps)	A_3	ΔE_3 (cm^{-1})	S_1 (cm^{-1}/ps)	S_2 (cm^{-1}/ps)	S_3 (cm^{-1}/ps)
W132	323.0	318.27	283.13	0	0	0	6.79	0.32	90.60	237.03	0.67	189.70	0	13.34	0.80
I5W	337.0	326.08	991.21	0.54	0.22	220.57	4.75	0.47	470.56	129.76	0.30	300.08	406.60	99.00	2.31
Y94W	338.5	326.58	956.06	0.37	0.43	414.74	5.52	0.38	361.78	163.97	0.19	179.55	1116.59	65.57	1.09
Y56W	341.5	322.66	1263.36	0.46	0.47	594.82	7.49	0.29	365.04	135.00	0.24	301.57	1297.85	48.72	2.23
S97W	344.3	323.76	1597.63	0.46	0.44	695.63	3.36	0.36	568.78	120.00	0.21	333.22	1522.70	169.30	2.78
T172W	344.5	324.02	1431.82	0.54	0.48	688.82	4.05	0.34	482.55	109.80	0.18	260.44	1275.94	119.04	2.37
R148W	346.0	325.03	1641.51	0.41	0.52	854.65	5.64	0.31	506.52	140.51	0.17	280.35	2084.50	89.81	2.00
N50W	349.5	327.55	1735.80	0.48	0.51	885.20	3.42	0.32	550.58	180.23	0.17	300.02	1836.57	161.05	1.66
N73W	349.5	324.97	1708.91	0.36	0.46	779.73	3.53	0.28	472.80	145.55	0.27	456.38	2157.76	134.10	3.14

λ_{SS}: steady-state fluorescence emission peak; λ_0: overall fluorescence emission peak at time zero; ΔE_{SS}: total Stokes shift; τ_1: decay constant of the first relaxation; A_1: relative contribution of the first relaxation to the total Stokes-shift; ΔE_1: Stokes shift by the first relaxation component; τ_2: decay constant of the second relaxation; A_2: relative contribution of the second relaxation to the total Stokes-shift; ΔE_2: Stokes shift by the second relaxation component; τ_3: decay constant of the third relaxation; A_3: relative contribution of the third relaxation to the total Stokes-shift; ΔE_3: Stokes shift by the third relaxation component; S_1: solvation speed for the first relaxation S_2: solvation speed for the second relaxation; S_3: solvation speed for the third relaxation.

Table S2. Fitting results of anisotropy dynamics and nuclear spin relaxation of all 9 mutants of γM7

Mutant	λ_{SS} (nm)	A_{2W}	τ_{2W} (ps)	A_{3W}	τ_{3W} (ps)	S^2	τ_{loc} (ns)	θ_{2W} (deg)	ω_{2W} (deg/ps)	θ_{3W} (deg)	θ_{NSR} (deg)	ω_{3W} (deg/ps)	ω_{NSR} (deg/ps)
W132	323.0	0.023	28.13	0.009	745.98	0.90	0	9.42	0.33	10.593	15.35	0.014	0
I5W	337.0	0.012	18.80	0.0092	612.14	0.76	1.47	11.51	0.61	10.51	24.45	0.017	0.017
Y94W	338.5	0.005	7.12	0.005	287.12	NaN	NaN	5.88	0.83	5.98	NaN	0.021	NaN
Y56W	341.5	0.013	13.19	0.016	545.93	0.77	1.47	10.52	0.80	12.14	23.67	0.022	0.016
S97W	344.3	0.018	10.14	0.010	173.01	0.69	0.92	11.55	1.14	9.26	28.23	0.054	0.031
T172W	344.5	0.012	19.80	0.043	600.00	NaN	NaN	11.16	0.56	24.97	NaN	0.042	NaN
R148W	346.0	0.022	18.30	0.023	411.27	NaN	NaN	13.29	0.73	14.86	NaN	0.036	NaN
N50W	349.5	0.019	14.99	0.013	222.43	0.75	0.81	14.052	0.94	12.33	24.74	0.055	0.031
N73W	349.5	0.027	13.75	0.020	352.49	0.52	1.32	16.74	1.22	16.26	36.66	0.046	0.028

λ_{SS}: steady-state fluorescence emission peak; λ_0: overall fluorescence emission peak at time zero; A_{2W}: relative contribution of the second relaxation to the total anisotropy; τ_{2W}: decay constant of the second relaxation; A_{3W}: relative contribution of the third relaxation to the total anisotropy; τ_{3W}: decay constant of the third relaxation; S^2: order parameter for the nuclear spin relaxation; τ_{loc}: local decay constant of nuclear spin relaxation; θ_{2W}: semi-angle of the first wobbling motion of Trp probe; ω_{2W}: angular velocity of the first wobbling motion of the Trp probe; θ_{3W}: semi-angle of the second wobbling motion of Trp probe; θ_{NSR}: semi-angle of the wobbling motion of the ^{1}H-^{15}N bond vector; ω_{3W}: angular velocity of the second wobbling motion of the Trp probe; ω_{NSR}: angular velocity of the second wobbling motion of the ^{1}H-^{15}N bond vector. NaN values were not measured by the NMR NSR technique

Table S3. Average number of water molecules within distance of indole ring for all 9 mutants of γM7.

Mutant	10 Å from Trp	7 Å from Protein	5 Å from Protein	5 Å from Trp
I5W	106.2	96.2	72.7	10.1
N50W	159.9	122.4	80.9	23.0
Y56W	84.6	83.4	73.0	12.0
N73W	168.0	127.0	83.9	27.2
Y94W	94.0	82.4	60.8	11.0
Y97W	147.0	115.0	76.5	19.6
W132	38.3	38.3	38.3	0.05
R148W	99.3	90.8	71.9	19.0
T172W	138.3	121.6	92.1	19.1

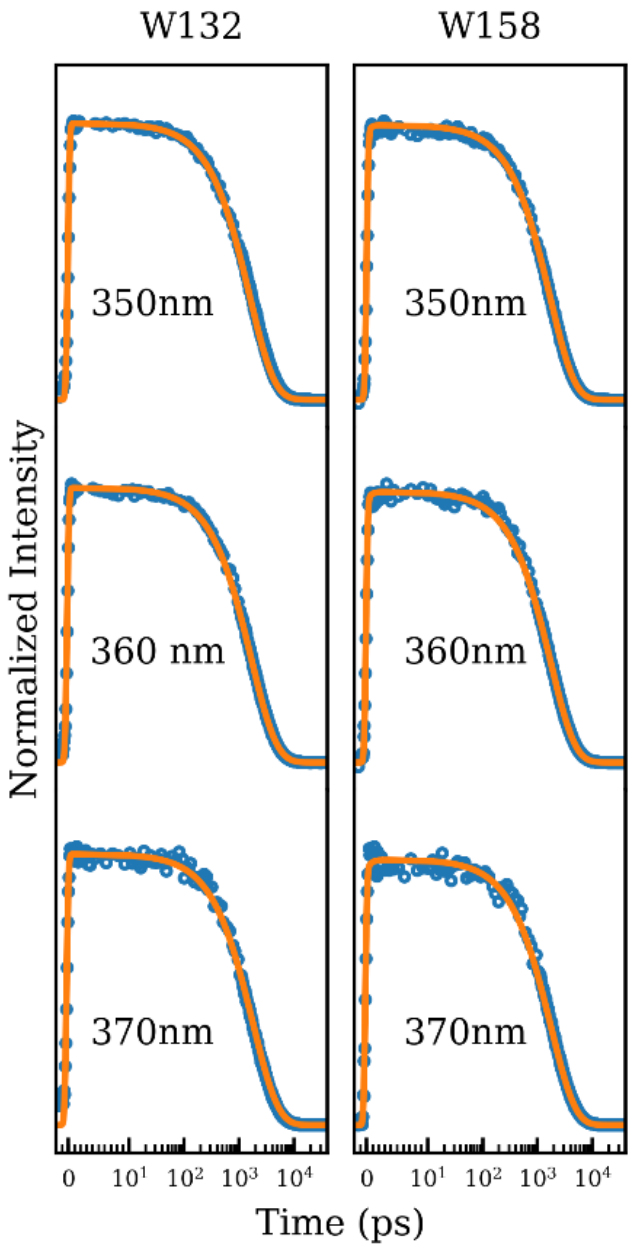

Figure S1. Comparison of transients from 350-370 nm for both intrinsic, buried tryptophan residues, W132 (left) and W158 (right). Blue markers represent experimental data and orange lines represent multi-exponential fits. Note that all decays are at the nanosecond time scale, typical for tryptophan lifetimes, and that we see no sub-nanosecond decay from electron transfer.

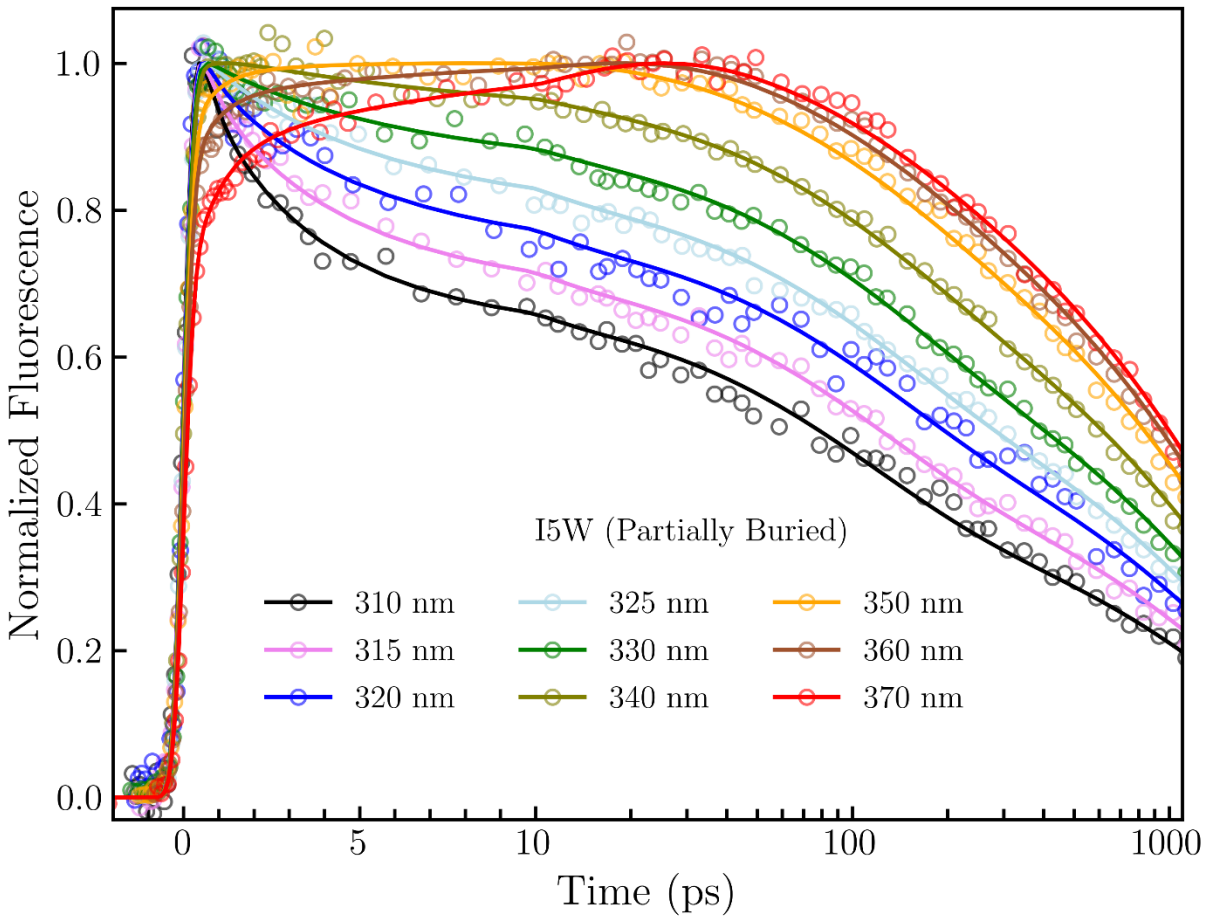

Figure S2 Normalized fluorescent transients gated from blue to red side of the emission spectrum of I5W.

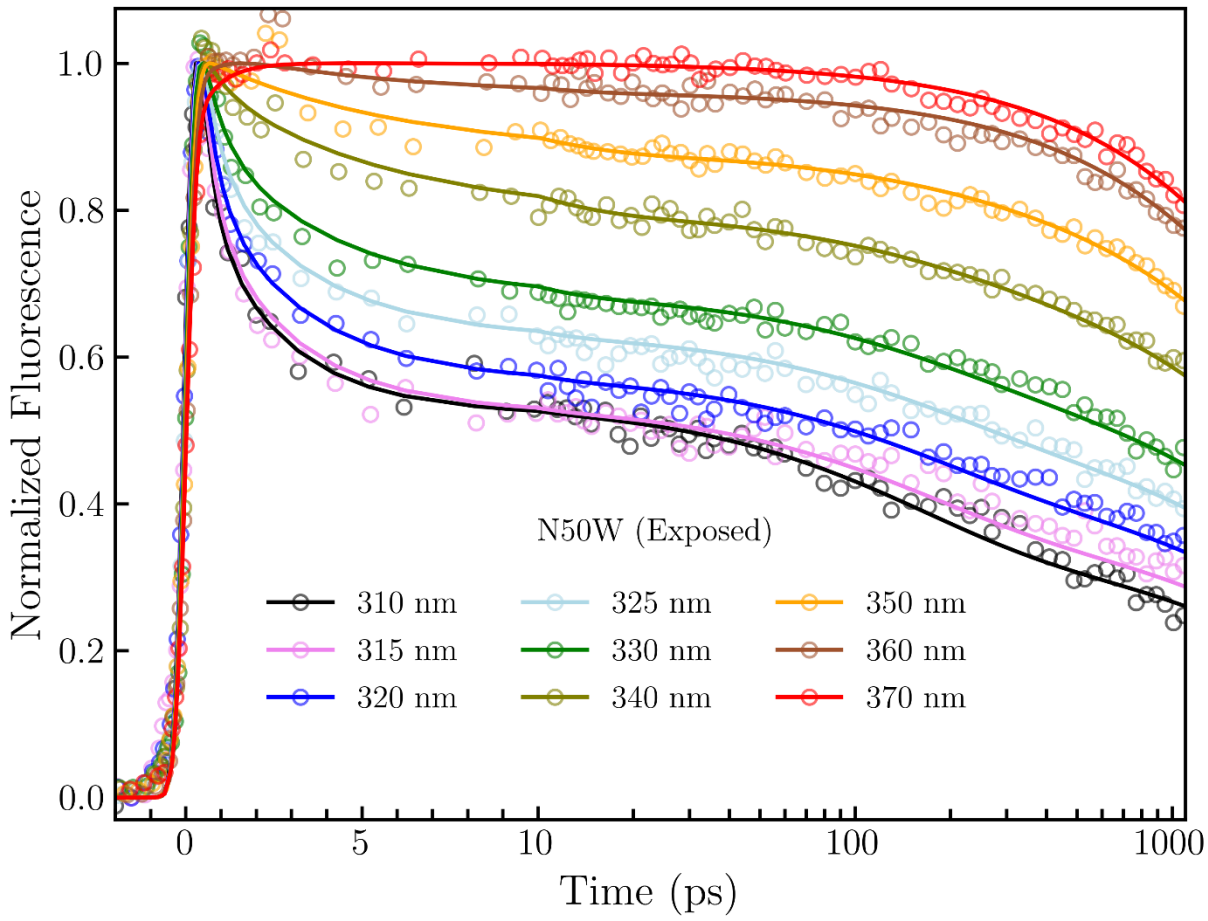

Figure S3. Normalized fluorescent transients gated from blue to red side of the emission spectrum of N50W.

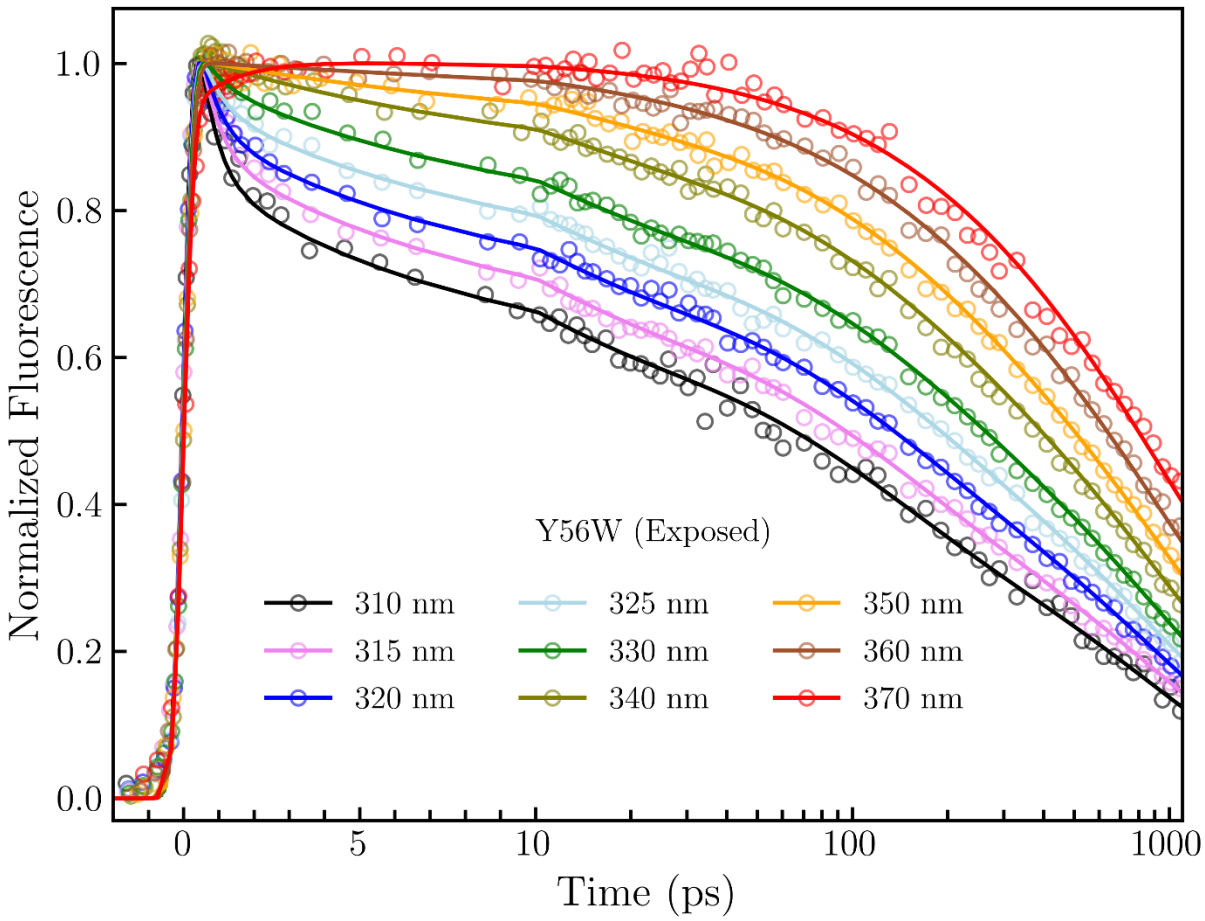

Figure S4. Normalized fluorescent transients gated from blue to red side of the emission spectrum of Y56W.

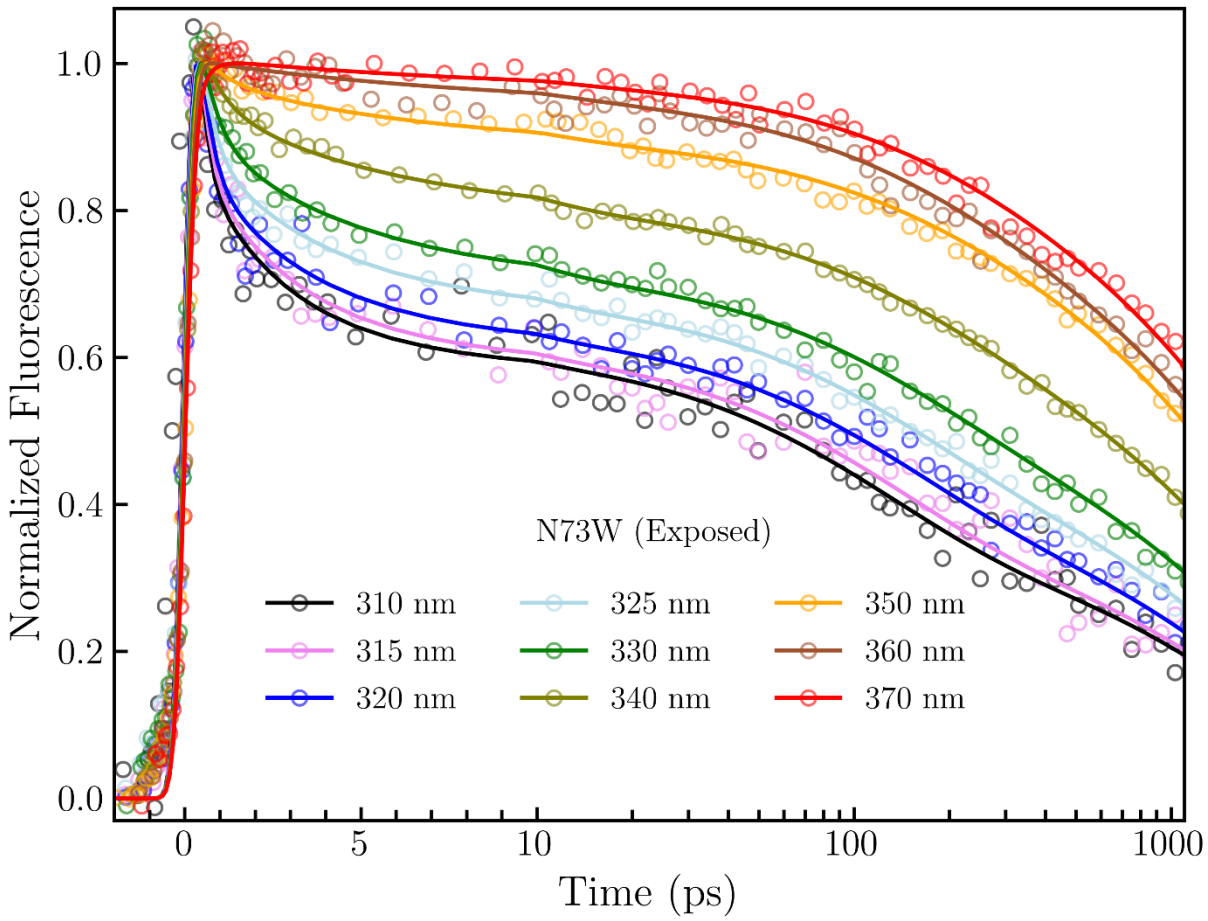

Figure S5. Normalized fluorescent transients gated from blue to red side of the emission spectrum of N73W.

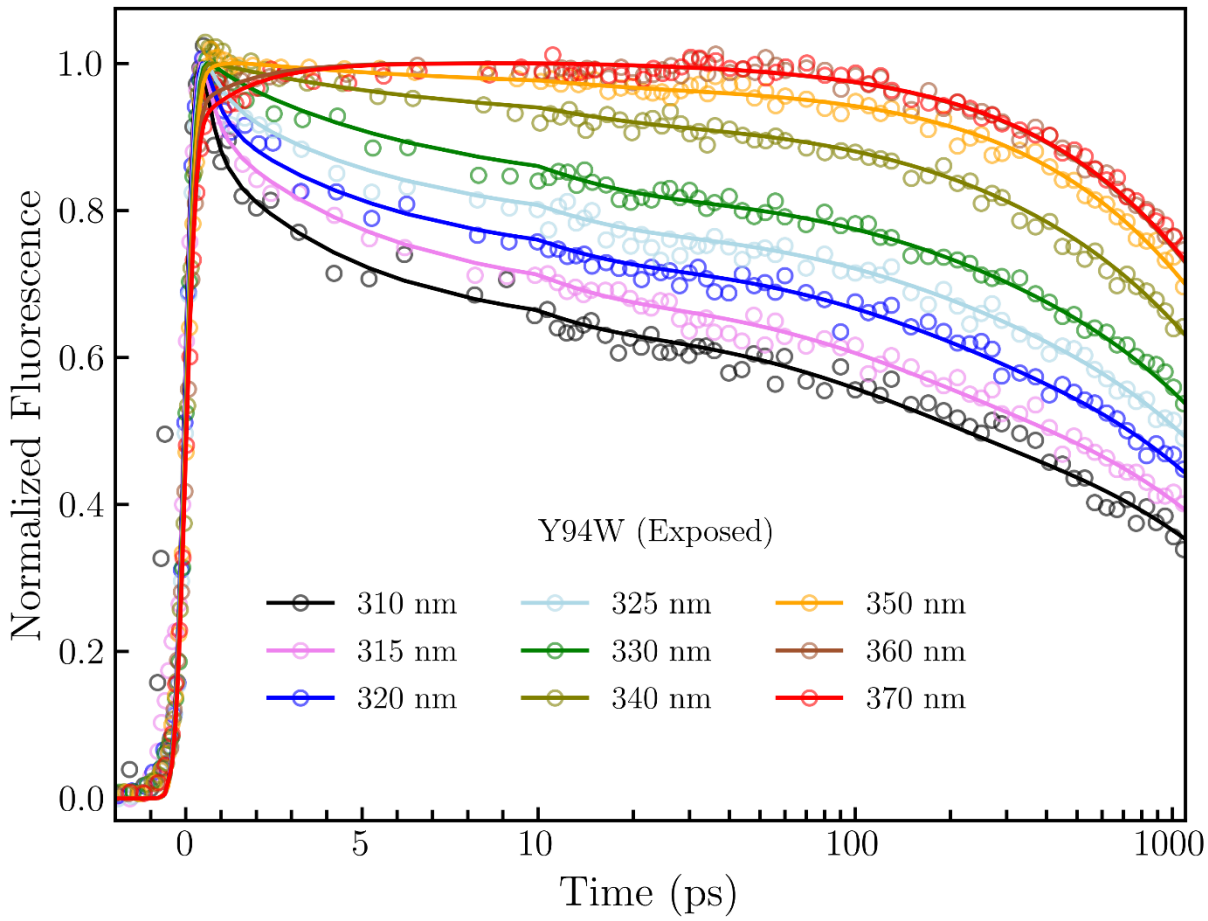

Figure S6. Normalized fluorescent transients gated from blue to red side of the emission spectrum of Y94W.

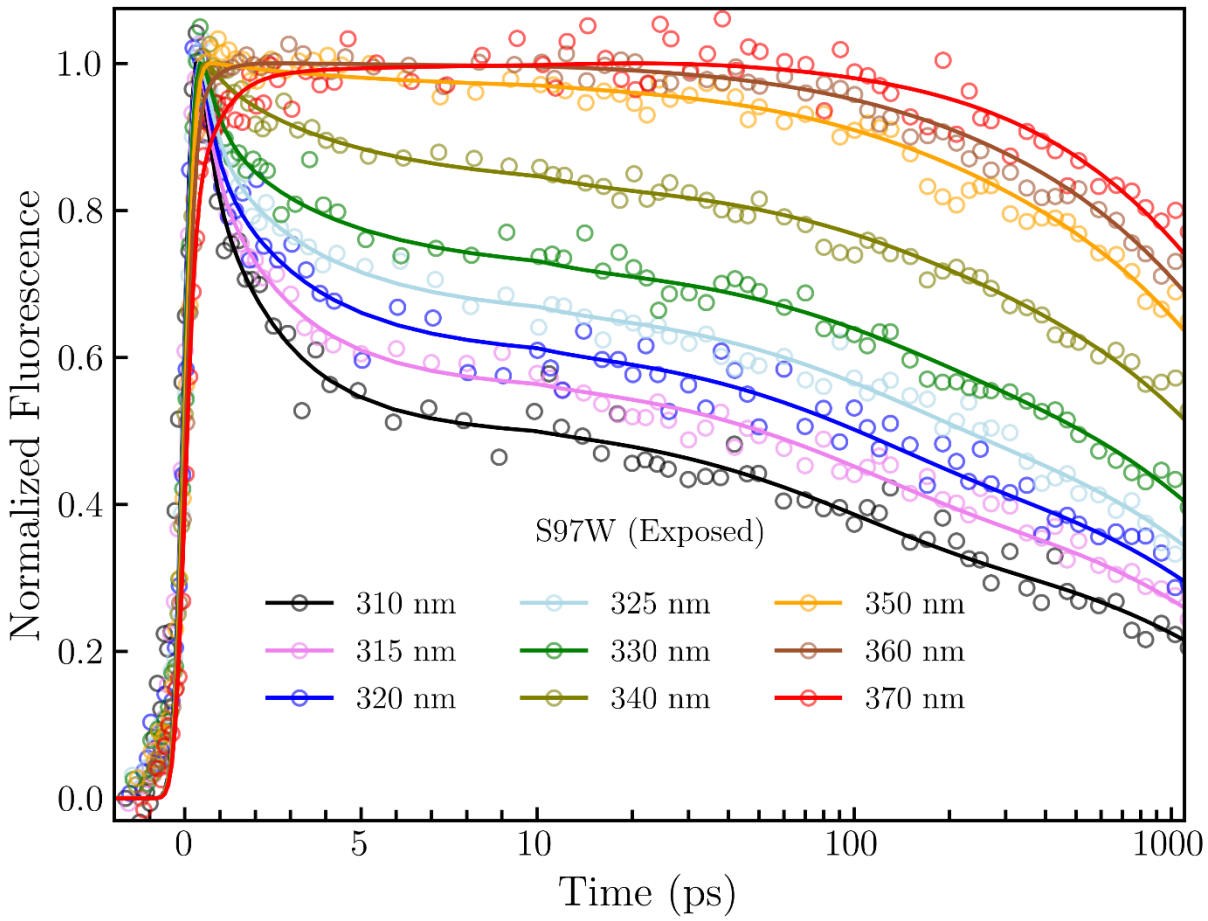

Figure S7. Normalized fluorescent transients gated from blue to red side of the emission spectrum of S97W.

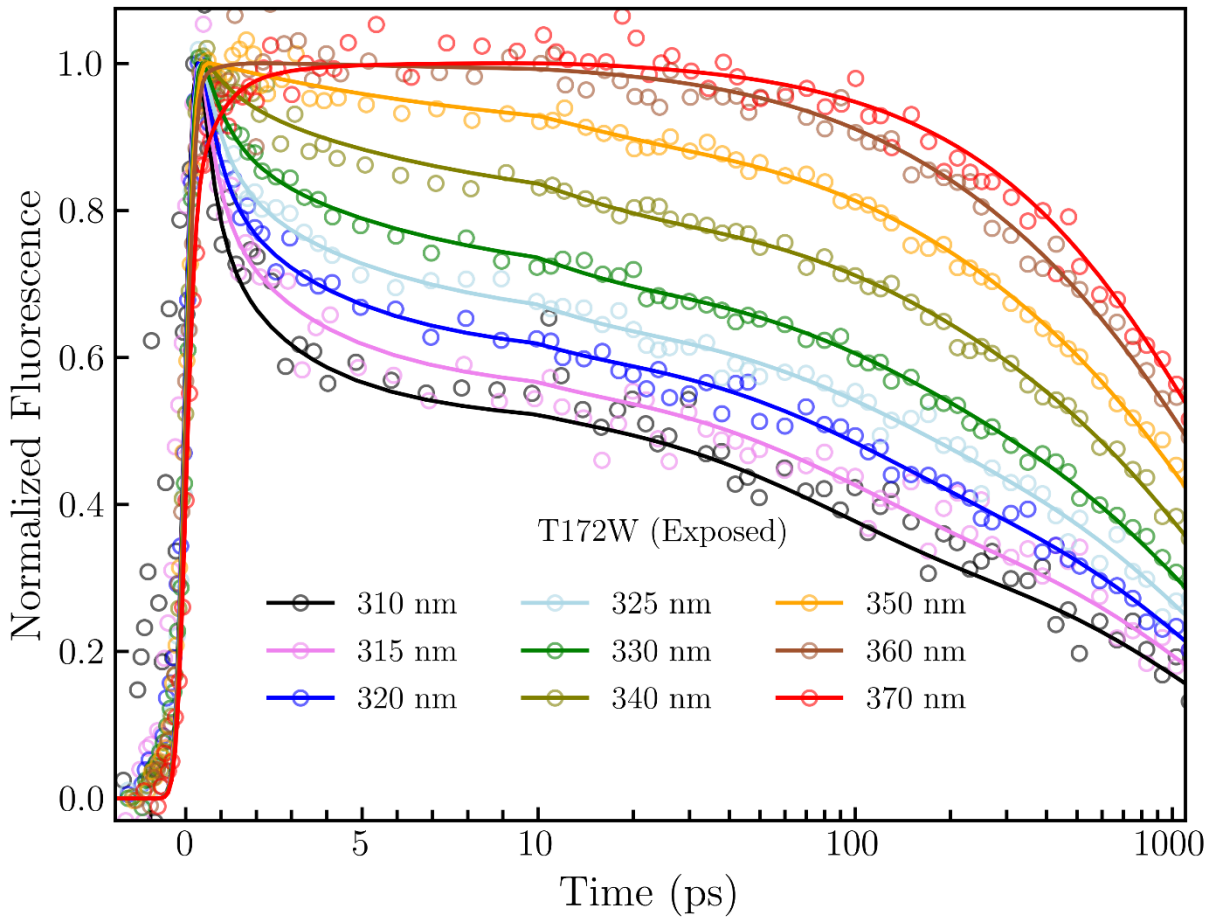

Figure S8. Normalized fluorescent transients gated from blue to red side of the emission spectrum of T172W.